Development 126, 5833-5846 (1999)
Printed in Great Britain © The Company of Biologists Limited 1999
DEV8655

A role for PS integrins in morphological growth and synaptic function at the postembryonic neuromuscular junction of *Drosophila*

Kelly J. Beumer[1], Jeffrey Rohrbough[1], Andreas Prokop[2] and Kendal Broadie[1,*]

[1]Biology Department, University of Utah, 257 S. 1400 E., Salt Lake City, UT 84112, USA
[2]Universität Mainz, Institut für Genetik – Zellbiologie, Becherweg 32, D-55128 Mainz, Germany
*Author for correspondence (e-mail: broadie@biology.utah.edu)

Accepted 5 October; published on WWW 24 November 1999

SUMMARY

A family of three position-specific (PS) integrins are expressed at the *Drosophila* neuromuscular junction (NMJ): a beta subunit (βPS), expressed in both presynaptic and postsynaptic membranes, and two alpha subunits (αPS1, αPS2), expressed at least in the postsynaptic membrane. PS integrins appear at postembryonic NMJs coincident with the onset of rapid morphological growth and terminal type-specific differentiation, and are restricted to type I synaptic boutons, which mediate fast, excitatory glutamatergic transmission. We show that two distinctive hypomorphic mutant alleles of the β subunit gene *myospheroid* (*mys*^{b9} and *mys*^{ts1}), differentially affect βPS protein expression at the synapse to produce distinctive alterations in NMJ branching, bouton formation, synaptic architecture and the specificity of synapse formation on target cells. The *mys*^{b9} mutation alters βPS localization to cause a striking reduction in NMJ branching, bouton size/number and the formation of aberrant 'mini-boutons', which may represent a developmentally arrested state. The *mys*^{ts1} mutation strongly reduces βPS expression to cause the opposite phenotype of excessive synaptic sprouting and morphological growth. NMJ function in these mutant conditions is altered in line with the severity of the morphological aberrations. Consistent with these mutant phenotypes, transgenic overexpression of the βPS protein with a heat-shock construct or tissue-specific GAL4 drivers causes a reduction in synaptic branching and bouton number. We conclude that βPS integrin at the postembryonic NMJ is a critical determinant of morphological growth and synaptic specificity. These data provide the first genetic evidence for a functional role of integrins at the postembryonic synapse.

Key words: Integrin, Neuromuscular junction, *Drosophila*, Synapse specificity

INTRODUCTION

Integrins have long been known to participate in embryonic neurogenesis. Integrin expression in the nervous system correlates with axonal outgrowth, target recognition and sprouting of synaptic arbors (Chiba and Keshishian, 1996; Martin et al., 1996). In recent years, integrins have also been implicated in postembryonic neuronal function. For example, integrins have been shown to participate in the mechanical modulation of neurotransmitter release in mature frog motor nerve terminals (Chen and Grinnell, 1995). Moreover, at least 10 different integrin subunits are expressed in the adult vertebrate brain (Pinkstaff et al., 1999). Functionally, the pharmacological blocking of integrins in rat hippocampal slices interferes with the stabilization of long-term potentiation (LTP), thought to form a mechanistic basis for learning and memory (Staubli et al., 1990). Genetic evidence suggests that a similar mechanism is essential for behavior regulation in *Drosophila* since mutations in an α integrin, *Volado*, cause defects in memory formation and retention (Grotewiel et al., 1998). Thus, integrins appear to play multiple roles in synaptic development and perhaps in the maintained developmental potential, or synaptic plasticity, believed to underlie behavioral modulation.

A great deal has been learned about the role of integrins in vertebrate neuronal development and function by studying in vitro preparations. For example, early in synaptogenesis, integrin-cytoskeleton interactions in growth cones are involved in stabilizing intercellular contacts (Schmidt et al., 1995). Following target recognition, integrins interact with laminin and agrin in neurally induced acetylcholine receptor clustering in the postsynaptic membrane (Burkin et al., 1998). However, in vivo confirmation of these mechanisms using genetic analyses has proven difficult, and genetic studies in mice often contradict in vitro results using pharmacological perturbation of integrin function (reviewed in Fassler et al., 1996; Hynes, 1996). These discrepancies might be due to the expression of multiple, potentially redundant, integrin subunits during vertebrate neurogenesis (Martin et al., 1996). However, removal of integrin subunits in less redundant invertebrate systems such as *C. elegans* and *Drosophila* has so far also revealed only minor defects in pathfinding, fasciculation and embryonic synaptogenesis (Baum and Garriga, 1997; Huang et al., 1998; Prokop et al., 1998). The question remains, therefore,

whether integrins play only subtle, minor roles during synaptic development or whether we have so far failed to appropriately assess the in vivo significance of this class of proteins.

An attractive model to further the genetic analysis of integrin synaptic function is the *Drosophila* neuromuscular junction (NMJ). This system is a powerful genetic model to analyze synaptic growth and transmission properties regulated through electrical activity, adhesion and signaling molecules (Chiba and Keshishian, 1996). Importantly, only five integrin subunits have been identified in *Drosophila*, two β (βPS and βν) and three α subunits (αPS1, αPS2, αVolado/scab/αPS3), and numerous mutant alleles of these integrin subunits are available (Brown, 1993; Grotewiel et al., 1998; Yee and Hynes, 1993). This relatively simple integrin complement contrasts favorably with the complex situation in vertebrates**.** We report here that the βPS, αPS1 and αPS2 integrin subunits become detectable at *Drosophila* NMJs during first and second larval instars, correlating with the onset of extensive morphological and physiological remodeling at the NMJ (Keshishian et al., 1996). Analyses of larvae carrying regulatory mutations affecting βPS expression or transgenic βPS constructs reveal that integrins impact morphological growth, synaptic specificity and, in some terminals, synaptic function, at the postembryonic terminal. These results provide the first genetic evidence that integrins are involved in postembryonic synaptic development and suggest that integrins may well play an important role in the modulatory mechanisms underlying synaptic plasticity.

MATERIALS AND METHODS

Fly stocks

Drosophila melanogaster stocks were reared at 25°C unless otherwise noted. Stocks were raised in well-yeasted, uncrowded vials on standard medium (Ashburner, 1989). Oregon-R flies were used as control animals. Three *myospheroid* (*mys*) mutant stocks were used: *sn v mys*^{b9} (D. Brower; see Flybase, 1998), a hypomorphic mutant that shows temperature-sensitive viability (D. Brower, personal communication), *cm ct*^{6} *mys*^{ts1}, also a weak hypomorphic mutant (Bunch et al., 1992); *mys*^{XG43}, an embryonic lethal genetic null (Bunch et al., 1992). For heat-shock overexpression, we used transgenic lines carrying P[HSPSβ] (Brabant and Brower, 1993). The construct was continually induced from hatching to late 3rd instar by a 50 minute heat-shock pulse at 37°C every 7 hours in a cycling incubator. Neural overexpression was induced using a P[UASβPS] construct (M. Brabant; constructed by M. Diamond) induced by a variety of previously described and newly isolated GAL4 constructs (Flybase, 1998). See Lindsley and Zimm (1992) for descriptions of the marker mutations used.

Immunocytochemistry

Wandering 3rd instar larvae were dissected and stained as previously reported (Broadie and Bate, 1993). To examine NMJ morphology, preparations were probed with a mouse monoclonal anti-cysteine string protein (CSP) antibody at 1:200 (Zinsmaier et al., 1990; K. Zinsmaier). Staining was visualized using a Vectastain ABC Elite kit with $NiCl_2$ or $CoCl_2$ enhancement and specimens mounted in Araldite (Broadie and Bate, 1993). Images were captured with an Optronics video camera and a Scion LG3 capture card. For clarity, different focal planes were occasionally combined in one picture using Adobe Photoshop 4.0.

In confocal preparations, either rabbit anti-DLG (discs-large, 1:1000; Woods and Bryant, 1991; D. Woods) or the mouse anti-CSP was used to mark synaptic arbors. Integrin expression was examined with the following antibodies: mouse monoclonal anti-βPS integrin antibody CF6G11 (1:500) or the CF6G11 ascites (1:300, both; Brower et al., 1984; N. Brown); mouse monoclonal anti-αPS1 antibody DK.1A4 (1:200) or mouse ascites anti-αPS1 antibody (1:500, both; Brower et al., 1984; D. Brower and E. Martín-Blanco, respectively); rat polyclonal anti-αPS2, PS2hc2 (1:5; Bogaert et al., 1987) and rabbit rabPS21 (1:1000; Bloor and Brown, 1998; N. Brown); rabbit polyclonal βν 84E (1:600; Yee and Hynes, 1993; R. Hynes). All anti-integrin antibodies were independently tested for their well-characterized embryonic staining patterns prior to probing the larval preparations (Bloor and Brown, 1998; Brower et al., 1984). Fluorescent secondaries used were Alexa-red-594- and Alexa-green-488-conjugated goat anti-mouse and goat anti-rabbit (Molecular Probes). Confocal microscopy was performed on a Bio-Rad MRC-600. NIH Image software was used to quantify staining intensity. Statistical significance of all measurements was determined with the Mann-Whitney-U test using InStat software except for the significance of synaptic specificity, which was determined with Fishers Exact test using InStat software.

Ultrastructural analysis

Flat dissected larvae (Broadie and Bate, 1993) were fixed for 10-60 minutes with 2.5% glutaraldehyde in 0.2 M phosphate buffer (pH 7.2). Fixation for immunoelectron microscopy: (a) 1 hour 4% paraformaldehyde in phosphate-buffered saline (PBS; 0.02 M phosphate buffer, 0.1 M NaCl, pH 7), wash in PBS-TX (0.1% Triton-X in PBS), normal antibody procedure (see above; sometimes with $NiCl_2$ enhancement); (b) 10 minutes 1% glutaraldehyde in 0.2 M phosphate buffer (pH 7-7.2), antibody procedure as above but without detergent (instead 0.2 M phosphate buffer). En bloc treatment, embedding, sectioning and microscopy as described previously (Prokop et al., 1998).

Micrographs showing boutons with active zones on muscle fibers 6/7 were taken randomly for statistical measurements. For size and area measurements, outlines of the particular structures were drawn onto transparencies, scanned into a computer, and measured using the histogram function in Adobe Photoshop. Vesicle numbers per bouton area were measured excluding the areas containing mitochondria or axolemma. For SSR analysis, SSR areas (excluding the bouton) were measured, or the SSR area was divided by the bouton area in each sectional plane. Statistical significance of all data was determined by Mann-Whitney-U-test.

Electrophysiology

Nerve-evoked excitatory junctional currents (EJCs) were recorded at 18°C from muscle 6 or muscle 4 (segment A3) of wandering 3rd instar larvae using standard two-electrode voltage-clamp techniques as described previously (Rohrbough et al., 1999). Recordings were made in a modified standard *Drosophila* saline (Jan and Jan, 1976) composed of: 128 mM NaCl, 2 mM KCl, 1.5 mM $CaCl_2$, 4 mM $MgCl_2$, 5 mM trehalose, 70 mM sucrose, 5 mM Hepes; pH adjusted to 7.1 with NaOH. EJCs were evoked by stimulating the severed segmental nerve (0.5 milliseconds, 0.2 Hz) with a suction electrode filled with extracellular saline. The stimulation voltage was increased until transmission failures were abruptly replaced by all-or-none responses. In all but a few mutant cases (see Results), increasing the voltage slightly revealed a second, high-threshold input which abruptly increased the peak synaptic current by an additional 2-fold or more. The voltage was raised ~50% over this level to safely excite both inputs. At the peak of the EJC, the intracellularly recorded voltage deviated by no more than 2-3 mV from the command potential (–60 mV). Current signals were filtered at 0.5 kHz, digitized to disk and subsequently analyzed using PClamp6 acquisition hardware and software (Axon Instruments). EJC mean peak amplitude was determined for each animal by averaging 10-20 consecutive responses. Spontaneous miniature EJCs (mEJCs) were recorded

continuously in muscle 4, in 1.5 mM Ca^{2+} saline containing 0.1 μg/ml TTX, and analyzed as reported previously (Rohrbough et al., 1999).

RESULTS

PS integrins are expressed at the postembryonic neuromuscular junction

At the *Drosophila* larval NMJ, motor axons contact specific target muscles and form characteristic arborizations at defined locations on the muscle surface (Johansen et al., 1989). These arborizations consist of branches forming numerous varicosities (boutons) falling into two primary classes: glutamatergic type I boutons (2-5 μm diameter) innervate all muscles and mediate fast, excitatory transmission; octopaminergic type II boutons (~1 μm diameter) are found on a subset of muscles, and appear to have a primarily modulatory function (Johansen et al., 1989; Keshishian et al., 1996). Growth at all arbors is activity dependent (Budnik et al., 1990) and a number of molecules involved in regulating this morphological plasticity have been identified (Budnik et al., 1996).

We became intrigued about the possible function of integrins in morphological synaptic plasticity in this system due to the isolation of Volado, an α integrin subunit required for *Drosophila* memory (Grotewiel et al., 1998). Additionally, expression of one subunit, αPS2, at the NMJ had been briefly reported (Fernandes et al., 1996). To assay synaptic integrin expression, we probed larval preparations with specific antibodies against αPS1, αPS2, βPS and βν integrin subunits (Fig. 1A-C). The αPS1, αPS2 and βPS subunits were clearly detectable; only the βν subunit did not appear to be present in the NMJ (not shown). PS integrin expression was restricted to type I boutons in a halo surrounding an unlabeled center, suggesting primarily postsynaptic localization (Fig. 1A-C). In double-labeled confocal sections, αPS and βPS integrin staining overlapped anti-DLG (discs-large), a primarily postsynaptic marker, although the PS integrin expression appeared to be less uniform than the anti-DLG staining (Figs 2A, 3A,D). αPS1 integrin staining was consistently fainter and less extensive than αPS2 and βPS integrin staining (Figs 1C, 3D). In addition to the intense βPS localization at the NMJ, fainter staining was observed throughout the muscle. We interpret this to be

Table 1. Summary of localization and expression of PS integrins in wild-type and *mys* mutant NMJs

Integrin	Coding Gene	Expression wt	Expression mys^{b9}	Expression mys^{ts1}	Synaptic Site
βPS	*myospheroid*	++++	++	+	pre/post
βν	*βν*	N/P	N/P	N/P	N/P
αPS1	*multiple edidimous wings*	+++	+	+	post
αPS2	*inflated*	++++	++	++	post
αVolado	*Volado (scab)*	++	N/D	N/D	pre

Relative levels of expression are indicated by ++. In the synaptic site column, pre and post indicate, respectively, presynaptic and postsynaptic localization of each subunit. N/P, not present; N/D, not done.

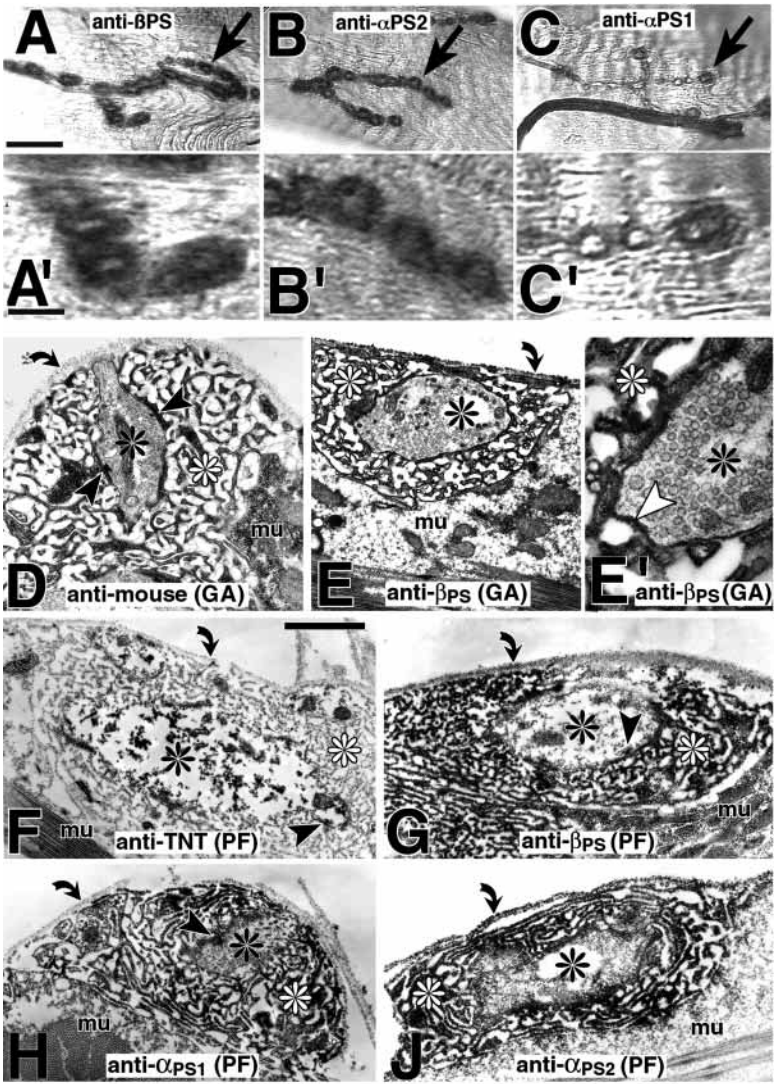

Fig. 1. Integrin expression at larval NMJs. (A-C) Characteristic staining patterns for anti-βPS, anti-αPS2 and anti-αPS1 at wild type 3rd instar NMJs on muscle 4 (magnified respectively in A′-C′). Arrows mark synaptic boutons. Staining intensity differs with the subunit but all show unstained boutons surrounded by a stained halo with the staining intensity highest at the inner edge and fading towards the outside. (D-J) Ultrastructural localization of integrins at the 3rd larval instar NMJ on muscles 6/7. Specimens were fixed in glutaraldehyde (GA) and treated without detergent (D,E,E′), or they were fixed in paraformaldehyde (PF) and treated with detergent (F-J). Presynaptic boutons (black asterisks) are filled with vesicles (visible only in D,E,E′), form synaptic release sites (black arrowheads; see Fig. 6), and are surrounded by SSR (white asterisks). Preparations are stained with (D) only secondary antibody, (E,E′,G) anti-βPS, (F) anti-Tetanus toxin in *C46;Uas-TetE* larvae, (H) anti-αPS1, and (J) anti-αPS2. Whereas in controls (D,F) the SSR is unstained, the SSR is strongly labeled by all integrin antibodies (D,E,E′,G-J). Anti-βPS staining deposit on the presynaptic membrane of boutons (white arrowhead in E′) suggests βPS integrin is also localized on the neuronal terminal. Curved arrows point at basement membrane on the muscle surface. Scale bar 20 μm (A-C), 5 μm (A′-C′), 370 nm (E), 1 μm (D,F-J).

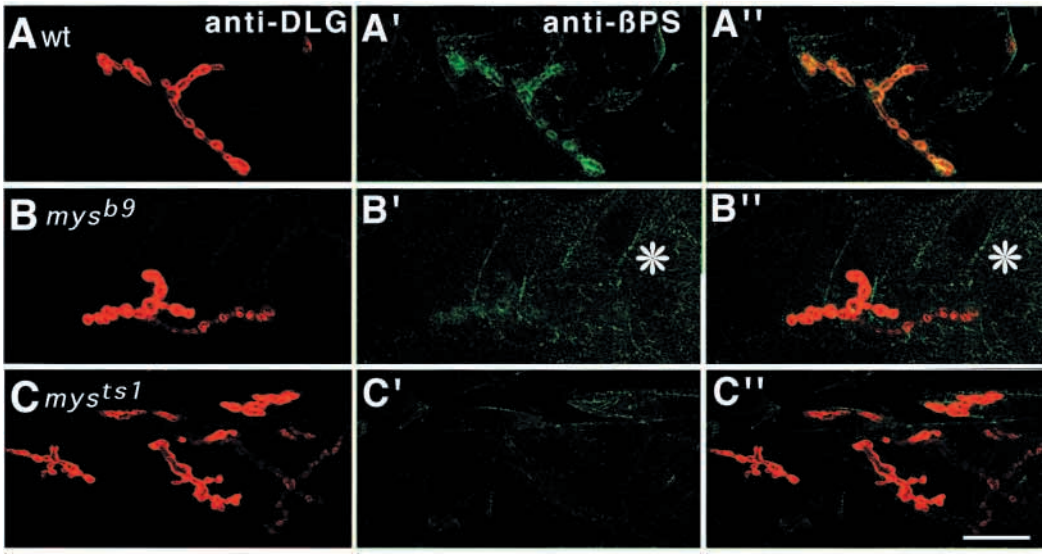

Fig. 2. βPS expression at *mys* mutant NMJs. Confocal images of larval muscle 4 NMJs double-labeled with anti-DLG (left column; A-C) and anti-βPS (A′-C′); overlap of both proteins appears yellow (merged image in right column; A″-C″). (A) Wild-type expression: anti-βPS overlaps the SSR marker anti-DLG; notice extrasynaptic staining of muscle surfaces (Volk et al., 1990). (B) In many undergrown mys^{b9} NMJs exhibiting βPS levels that are severely reduced, synaptic and extrasynaptic stains are indistinguishable (30% of muscle 4 NMJs); note increase of extrasynaptic staining (asterisk). (C) Severely overgrown mys^{ts1} NMJ lacking detectable anti-βPS expression; (80% of muscle 4 NMJs). Scale bar 25 μm.

sarcomeric expression of βPS dimerized with αPS2, as previously reported (Volk et al., 1990).

In order to localize PS integrins expression more precisely, mature larval NMJs were probed with anti-PS integrin antibodies and embedded for ultrastructural analysis (Fig. 1D-J). Antibody staining against αPS1, αPS2 and βPS integrin subunits, but not the control staining (Fig. 1D, F), all showed expression throughout the subsynaptic reticulum (SSR), a system of postsynaptic foldings of the muscle membrane that surrounds the presynaptic boutons in type I arbors (Budnik et al., 1996; Fig. 1D-J; Table 1). These results clearly confirm that all three PS integrins occur at least postsynaptically. In additional experiments, pre-embedding-anti-βPS staining could be achieved in the absence of detergent, thus preserving the cell membranes. In these specimens, unopposed presynaptic membranes often revealed staining deposits suggesting that at least βPS integrin is expressed in the presynaptic membrane in addition to the postsynaptic SSR (white arrowhead in Fig. 1E′; Table 1).

Developmentally, all three PS integrins become detectable at the NMJ in late 1st or early 2nd instar larvae, although others have reported earlier expression in the CNS (Hoang and Chiba, 1998). We were unable to detect expression in embryos or hatching 1st instar larvae in the peripheral nerves or NMJ, although the expected expression at the muscle attachment sites was clearly visible for all three subunits (not shown). Thus, PS integrin expression becomes concentrated at NMJs only after they have been differentiated and stabilized during embryogenesis. This late onset of expression coincides with the appearance of the SSR, the period when different morphological classes of NMJs first appear and the terminals first become subject to measurable activity-dependent morphological plasticity (Budnik, 1996; Keshishian et al., 1996).

Hypomorphic mutant alleles of *myospheroid* reduce PS integrin expression at the synapse

We next addressed potential functions of PS integrins at the *Drosophila* NMJ, focusing primarily on the βPS subunit. Because null alleles of *myospheroid* (*mys*), the gene encoding the βPS integrin subunit, cause embryonic lethality due to muscle detachment (Leptin et al., 1989), we characterized two viable, hypomorphic alleles, mys^{b9} and mys^{ts1}. These alleles encode and express structurally normal proteins as assayed on western blots, but show specific regulatory defects (Bunch et al., 1992; D. Brower, personal communication) and mys^{b9} shows incomplete late larval lethality at 29°C. Experiments were carried out at both 29°C and 25°C, but temperature did not appear to affect synaptic expression of the βPS protein or any of the observed NMJ phenotypes (see below).

Homozygous animals from both mutant strains were tested for alterations in expression of the βPS integrin subunit at the NMJ in wandering 3rd instar larvae (Table 1). βPS expression at both 29°C and 25°C was intense and reliably observed in all type I NMJs of normal larvae (Fig. 2A, n=97 terminals, 15 animals), but detected in just 50% of NMJs in mys^{b9} animals (n=106, 17 animals, Fig. 2B) and in only 20% of NMJs in mys^{ts1} larvae (n=136 terminals, 18 animals; Fig. 2C). Detectable expression ranged from nearly wild type to nearly background in both mutants. In both alleles, reduction in synaptic βPS expression followed a dorsoventral gradient with dorsal NMJs consistently less likely to stain above background (ventral muscles 6/7, ~70%; dorsolateral muscle 4, ~30%). However, the mechanistic cause for the reduction of synaptic protein levels in these alleles might be different, since extrasynaptic muscle expression appeared comparable to wild type in mys^{ts1} mutant larvae, but was reproducibly increased in mys^{b9} (Fig. 2B′). We conclude, therefore, that mys^{b9} causes an inappropriate distribution of the βPS protein, moderately reducing the frequency of detectable synaptic βPS expression (reduced 50%) while consistently upregulating extrasynaptic muscle expression, whereas mys^{ts1} strongly and specifically reduces the frequency of detectable βPS expression at the NMJ terminal (reduced 80%) with no detectable corresponding increase elsewhere in the muscle.

It is generally accepted that α and β integrins must

heterodimerize to be transported to the plasma membrane (Cheresh and Spiro, 1987). Since the βPS subunit is known to form heterodimers with the αPS1 and αPS2 subunits in other *Drosophila* tissues (Bogaert et al., 1987; Leptin et al., 1989), we tested whether reduced levels of βPS affect expression of αPS integrins at the NMJ (Table 1). Anti-αPS1 and anti-αPS2 immunostaining was detectable at all mutant NMJs, but was moderately reduced at mys^{b9} mutant NMJs and strongly reduced at mys^{ts1} mutant NMJs (Fig. 3). This observation strongly suggests that βPS dimerizes with both αPS1 and αPS2 at the NMJ. However, in both *mys* mutant alleles, αPS expression persists at a level higher than predicted if βPS was the sole β subunit. Therefore, we suggest that a novel β subunit may be present at the NMJ (Fig. 3; see Discussion).

NMJ morphological development is differentially altered in *mys* mutant larvae

The postembryonic onset and strictly localized synaptic expression of the PS integrins suggests that these proteins may play a specialized role in synaptic structural or functional modulation. We first asked whether the *mys* mutant alleles altered the NMJ synaptic architecture. We assayed the morphology of NMJs in abdominal segment A2 innervating muscle 4 (a simple terminal, i.e. having, on average, only two nerve inputs and low orders of branching), muscle 6 (a more complex terminal also having two inputs, but many more boutons and much more complex branching) and muscle 12 (the most complex terminal, i.e. having, on average, three or more inputs, and five or more primary branches with increased branching complexity). We quantified NMJ morphology on muscle 4 and muscle 12 by counting branches and boutons in A2. Due to the complexity of branching, and the compaction of all mutant muscle 6 NMJs, we counted boutons but did not attempt to quantify branching on muscle 6. A bouton was defined as a terminal varicosity expressing synaptic markers (e.g. vesicle-associated CSP) and an arboreal branch was defined as a terminal process consisting of at least two boutons. Bouton quantification was restricted to type I boutons, since type II terminals do not appear perturbed under these mutant conditions.

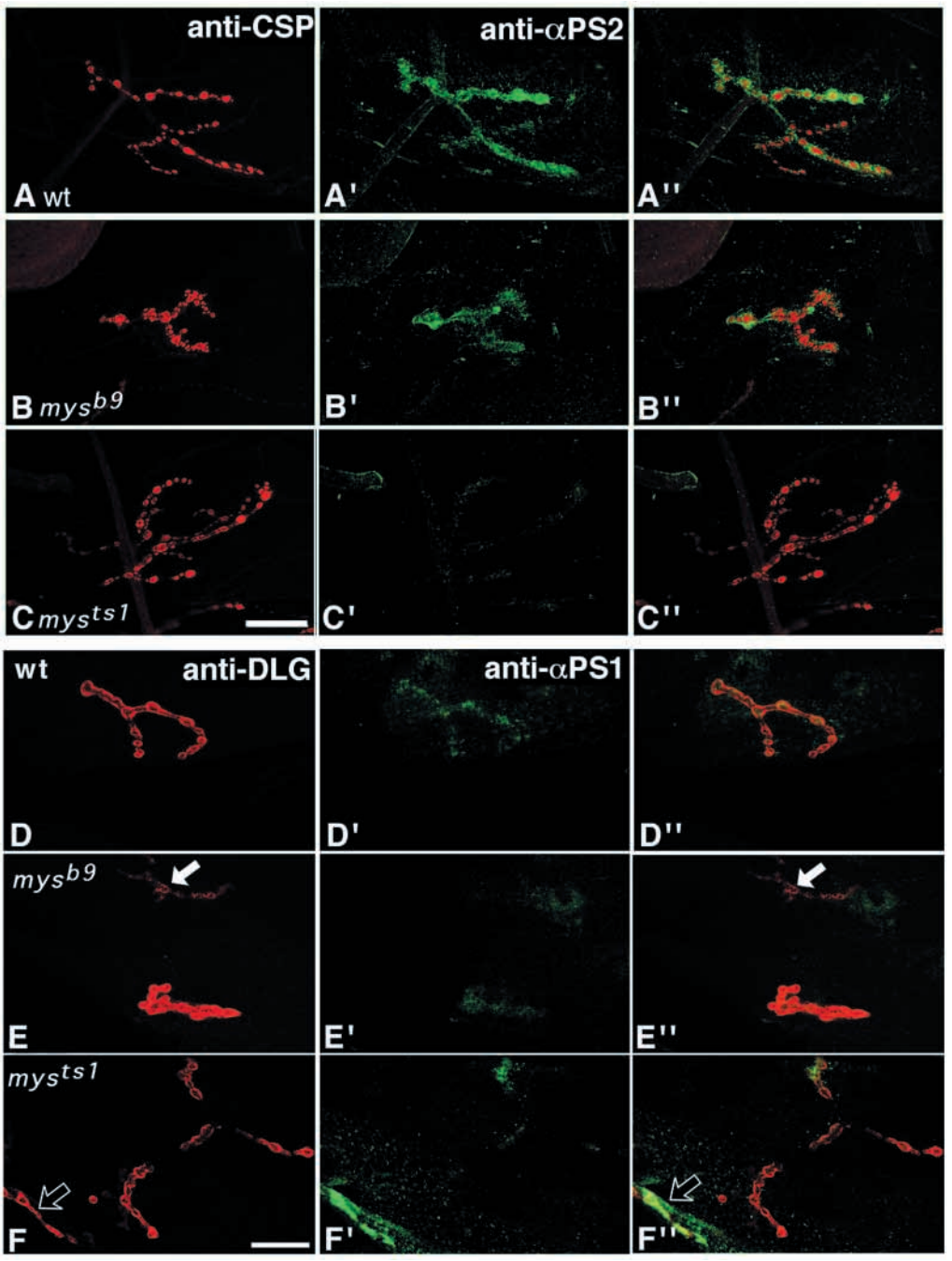

Fig. 3. αPS1 and αPS2 expression at wild-type and *mys* mutant NMJs. Confocal images of larval NMJs double labeled with (left column) anti-CSP (A-C) or anti-DLG (D-F), and (middle column) anti-αPS2 (A′-C′) or anti-αPS1 (D′-F′); overlap of both proteins appears yellow (merged image in right column; A″-F″). Anti-αPS2 staining is moderately reduced in mys^{b9} and strongly reduced in mys^{ts1} mutant junctions (B′,C′). (D′) Anti-αPS1 staining at wild-type NMJs is much weaker and grainier than either anti-βPS or anti-αPS2 (see also Fig. 1A-C) but overlaps comparably with anti-DLG staining (D″-F″). Most of the anti-αPS1 label is gone in the mys^{b9} and mys^{ts1} mutant junctions (E′,F′; notice a nonstaining junction in E,E″, white arrow, and a staining junction in F,F″, arrow). Scale bar 25 μm.

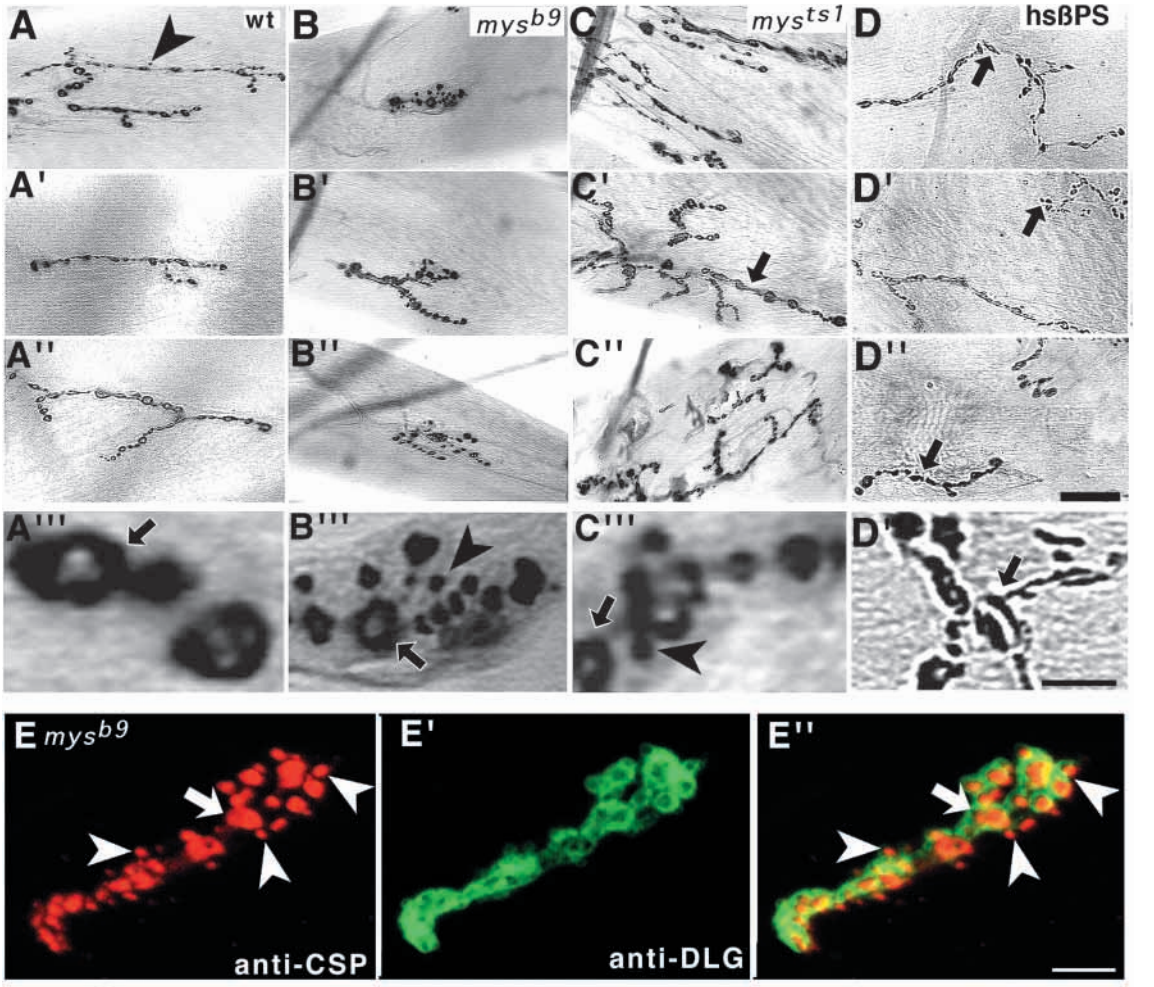

Fig. 4. *mys*^{b9}, *mys*^{ts1} and P[HSPSβ] mutant NMJs are affected in growth and morphology. Muscle 4 NMJ terminals in wild-type (A), *mys*^{b9} (B) *mys*^{ts1} (C), and P[HSPSβ] (D) larvae. Three examples each of typical terminals labeled with anti-CSP as a presynaptic terminal marker. (A) In wild-type terminals, varicosities are uniformly spaced, staining is uniform and boutons are large with stereotypical morphology. (B) Arbors in *mys*^{b9} mutants are smaller, with short branches and small, tightly clustered boutons. (C) Terminals in *mys*^{ts1} animals are overgrown and disordered. Boutons are often smaller and more widely spaced (arrow). (D) Terminals in P[HSPSβ] larvae are disordered and stain more faintly than wild type. Close ups of bouton morphology in wild-type larvae (A″), *mys*^{b9} (B″), *mys*^{ts1} (C″) and P[HSPSβ] (D‴). Mature type I boutons are reduced in size, but uniformly stained in the doughnut pattern characteristic of vesicle markers (black arrows). Immature mini-boutons are visible in the wild-type junction (arrowhead), but the number is dramatically increased in *mys* mutant NMJs. P[HSPSβ] boutons are small and abnormally shaped (arrows). (E) *mys*^{b9} muscle 4 NMJ labeled with anti-CSP (red; showing the presynaptic terminal) and anti-DLG (green; showing postsynaptic SSR). Both large (arrow) and mini-boutons (arrowhead) are surrounded with DLG-labeled SSR. Scale bar is 20 μm in A-D″, 4 μm in A‴-D‴ and 12 μm in E-E″.

Using the synaptic vesicle marker anti-CSP to visualize NMJs (Fig. 4), we observed that arboreal branches of all homozygous *mys*^{b9} mutant NMJs were dramatically shortened and synaptic boutons were both smaller and more tightly spaced than in wild-type animals, greatly reducing the synaptic terminal area (Fig. 4). In addition, mutant terminals contained abundant clusters of 'mini-boutons'; very small (<1 μm) boutons that are only infrequently observed in wild-type terminals (Fig. 4B-B″, arrowheads in E). Labeling with the SSR marker anti-DLG revealed the mini-boutons to be surrounded by SSR as is characteristic of type I boutons (Fig. 4E, arrowhead), and we therefore counted them as such; however, this inclusion undoubtedly artificially inflated the bouton quantification (see below), leading to an underestimate of the phenotype severity. In addition to these aberrant mini-boutons, even the 'mature' (i.e. >1 μm) type I boutons are significantly smaller in *mys*^{b9} than wild type (compare Fig. 4A‴ with B‴).

On both muscle 4 and muscle 12, *mys*^{b9} mutant terminals also showed a significant decrease in all orders of terminal branches, resulting in a very highly significant decrease in the total number of arboreal branches (Fig. 5A,B; $n \geq 17$ hemisegments per strain). As well, type I bouton numbers are very significantly reduced at NMJs on muscles 4, 6 and 12 (Fig. 5C). Thus, the undergrowth phenotype in *mys*^{b9} mutant larvae results in a compaction and simplification of the synaptic architecture, and reduction in size and number of type I boutons. This reduction is not related to a decrease in muscle

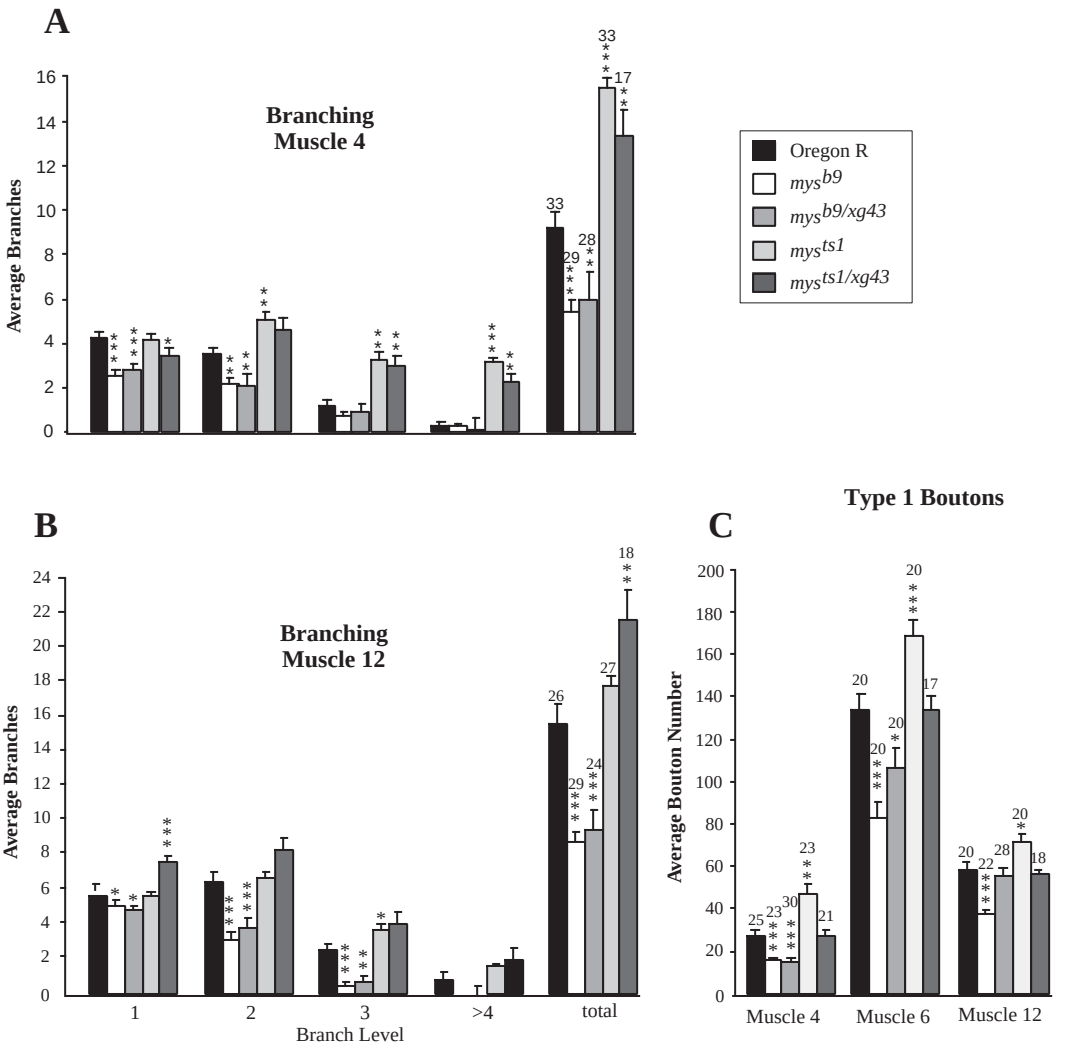

Fig. 5. Quantification of NMJ morphological features in muscle 4 (simple), 6 (intermediate) and 12 (complex) in *mys* mutant animals. NMJ terminal morphology was assayed in wild-type (Oregon R), mys^{b9}, mys^{b9}/mys^{XG43}, mys^{ts1}, mys^{ts1}/mys^{XG43} and P[HSPSβ] 3rd instar wandering larvae. (A,B) Branches on muscle 4 and 12, respectively. Branching is quantified from the first branches after axonal entry (1°) through the higher order branches (2-4°) and also as total number of synaptic branches present in the arbor. (C) Quantification of type I boutons on muscles 4, 6 and 12 in all four genotypes. Numbers indicate hemisegments scored. Error bars indicate S.E.M. Statistics were calculated with the Mann-Whitney U-test using Instat software (*, $P<0.05$; **, $P<0.01$; ***, $P<0.001$).

size, as all mutant genotypes showed no significant difference from wild type in muscle area. The average area of muscle 4 and muscle 12, respectively, were 1526±7.36 μm^2 and 846±5.30 μm^2 in OR controls, 1466±5.52 μm^2 and 796±3.88 μm^2 in mys^{b9} and 1564±7.88 μm^2 and 844±4.26 μm^2 in mys^{ts1}. These values do not significantly differ between genotypes (muscle 4, OR/mys^{b9}, P=0.0944, OR/mys^{ts1} P=0.7057; muscle 12, OR/mys^{b9}, P=0.5871, OR/mys^{ts1} P=0.8746). To confirm that these phenotypes were specific to the *mys* mutation, we also analyzed mys^{b9}/mys^{XG43} heterozygous animals (mys^{XG43} is a protein null; Fig. 5). NMJs in these animals also have small, tightly clustered boutons surrounded by numerous mini-boutons. Both bouton numbers and numbers of branches tend to increase slightly towards wild type; the significance of this increase is discussed below (see Discussion).

Homozygous mys^{ts1} mutant NMJs were significantly larger and more complex than normal, a phenotype opposite of mys^{b9} mutant NMJs (compare in Fig. 4). This striking overgrowth phenotype was similar in animals raised at 25°C and 29°C, and more obvious at the normally simpler muscle 4 terminal than at the more complex muscle 12 terminal. Although the number of primary NMJ branches (1°) on muscle 4 was normal, all higher order branching (>2°) was very significantly increased resulting in a highly significant increase in total branching (Figs 4C, 5A). This trend is less obvious on muscle 12, perhaps because this NMJ is already more complex in the wild type (Fig. 5B). As well, type I boutons in mys^{ts1} mutant NMJs were significantly increased on all scored muscles, in close agreement with the branching defects (Fig. 5C). Thus, the overgrowth phenotype in mys^{ts1} mutant larvae results in an elaboration of the synaptic architecture and an increase in type I boutons. However, when mys^{ts1}/mys^{XG43} heterozygous animals raised at 29°C were analyzed, although the branching phenotype was entirely consistent, these animals showed no significant increase in bouton numbers, indicating that the differentiation of boutons in these enlarged arbors may be a multigenic trait, influenced by the genetic background. Alternatively, changing the protein expression by placing a complex regulatory mutant over a null may change expression in unexpected ways, significantly affecting the observed phenotype (see Discussion).

In order to confirm the specificity of the phenotypes observed in both mutant strains, preparations were identified by genotype in a blind study. Out of 34 preparations, 32 were correctly identified. As complex morphological phenotypes tend to vary around a mean overlapping wild type, this

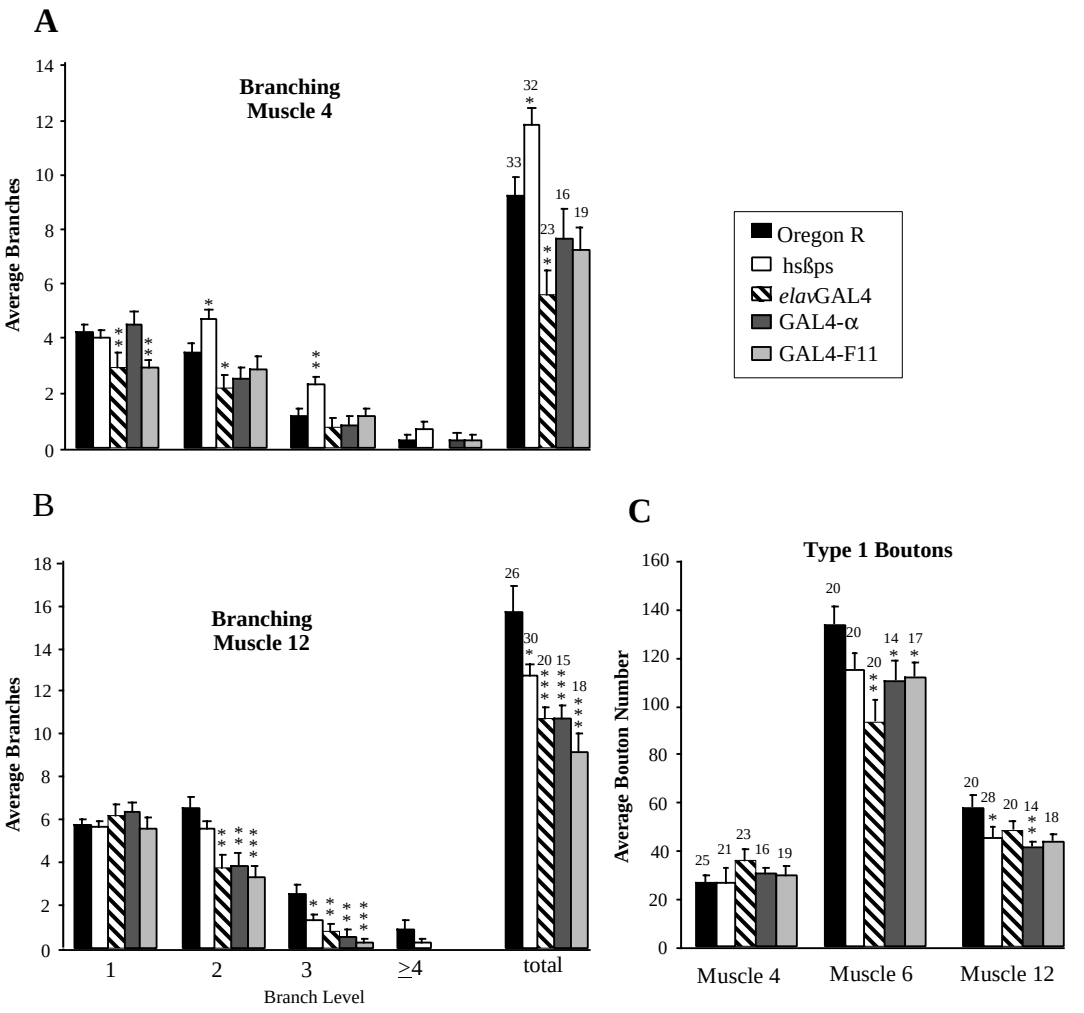

Fig. 6. Quantification of NMJ morphological features in muscle 4 (simple), 6 (intermediate) and 12 (complex) in βPS overexpression animals. Terminals were assayed in wild type (Oregon R), heat-shock ubiquitous overexpressing line (P[HSPSβ]), neuronal-specific overexpressing line (elavGAl4 /P[UASβPS]), and two muscle-specific overexpressing lines (GAL4-α /P[UASβPS], and GAL4-F11 /P[UASβPS]). (A,B) NMJ branches on muscle 4 and 12, respectively. Branching is quantified from the first branches after axonal entry (1°) through the higher order branches (2-4°) and also as total number of synaptic branches present in the arbor. (C) Quantification of type I boutons on muscles 4, 6. and 12 in all four genotypes. Numbers indicate hemisegments scored. Error bars indicate S.E.M. Statistics were calculated with the Mann-Whitney U-test using Instat software (*, $P<0.05$; **, $P<0.01$; ***, $P<0.001$).

indicates a highly reliable identification of the mutant phenotypes and confirms the qualitative severity of these NMJ growth defects in distinct *mys* regulatory mutants.

Overexpression of the βPS subunit reduces NMJ growth and complexity

Our results with the *mys* mutant alleles suggest that the level and/or distribution of PS integrin in the synaptic terminal is important for controlling NMJ sprouting and bouton formation. We tested this hypothesis by overexpressing the *mys* gene in wild-type animals and assaying effects on NMJ morphology. We used larvae carrying a heat-inducible *hsp70-mys* construct that has been shown to express βPS protein at a high enough level to rescue lethal mutant phenotypes (Brabant and Brower, 1993). Using the same induction-protocol as Brabant and colleagues (37°C heat shock every 7 hours from hatching to scoring) and quantifying βPS expression at the NMJ from confocal images using the NIH Image program, we observed a significant increase in βPS protein expression at the NMJ and throughout the muscle consistent with the observed phenotype.

Since the heat-inducible *hsp70* promoter is not cell or tissue specific, the βPS levels increased ubiquitously in all larval tissues. This overexpression caused larval and pupal lethality. Larvae that survived to wandering 3rd instar often undergo premature histolysis, complicating analyses of NMJ morphology. However, at a qualitative level, NMJs of heat-shocked larvae were clearly structurally disordered, with reduced branches and smaller, abnormally shaped boutons (Fig. 4D). The simple muscle 4 terminals showed no significant quantifiable alterations in the number of synaptic branches or type I boutons (Fig. 6A,C), perhaps owing to the starting simplicity of this junction. In contrast, the complex muscle 12 terminals showed a significant decrease in the number of total synaptic branches, resulting primarily from a loss of higher order branches (≥3°; Fig. 6B) and a highly significant decrease in the number of type I boutons (Fig. 6C). Wild-type controls subjected to the same protocol were qualitatively and quantitatively normal (not shown). Thus, ubiquitous overexpression of βPS causes an undergrowth phenotype similar to that observed at mys^{b9} mutant NMJs, as well as abnormal bouton morphology. We note that both mys^{b9} and the hs-construct cause an increase in βPS expression in extrasynaptic regions of the muscle.

To clarify the results observed with ubiquitous βPS overexpression, we next induced overexpression with GAL4 insertions with expression patterns specific to either nerve or muscle tissue (Fig. 6). When βPS expression was induced in all neural tissue throughout development using *elavGAL4*

(Flybase, 1998), branching and bouton numbers were again significantly reduced in all NMJs. However, a very intriguing observation was that bouton morphology was normal and there was no increase in mini-boutons. A similar result was seen using two muscle-specific GAL4s, GAL4-α and GAL4-F11 (Fig. 6), which begin muscle expression during early 2nd instar. In both cases, bouton number and branching defects at all NMJs were consistent with the results observed with hsβPS – significantly decreased at muscles 6 and 12, with branching, but not bouton numbers reduced at muscle 4 (Fig. 6). Additionally, muscle-specific βPS overexpression caused a moderate increase in mini-boutons (not shown). Thus, overexpression of βPS in neural and/or muscle tissue results in reductions in both branching and bouton differentiation at NMJs on muscles 6 and 12, and in a loss of branching, but not boutons, on muscle 4. Early muscle βPS overexpression results in an increase in mini-boutons.

In summary, our results show that regulated levels of PS integrin expression in synaptic and extrasynaptic regions of the NMJ synaptic arbor are required as promoting and inhibiting growth regulators of morphological growth and bouton differentiation. The expression of βPS in the membranes of both synaptic partners plays a key role in the regulation of growth. One important conclusion is that elevated extrasynaptic βPS may serve to inhibit growth and arrest nascent boutons in a developmentally immature state.

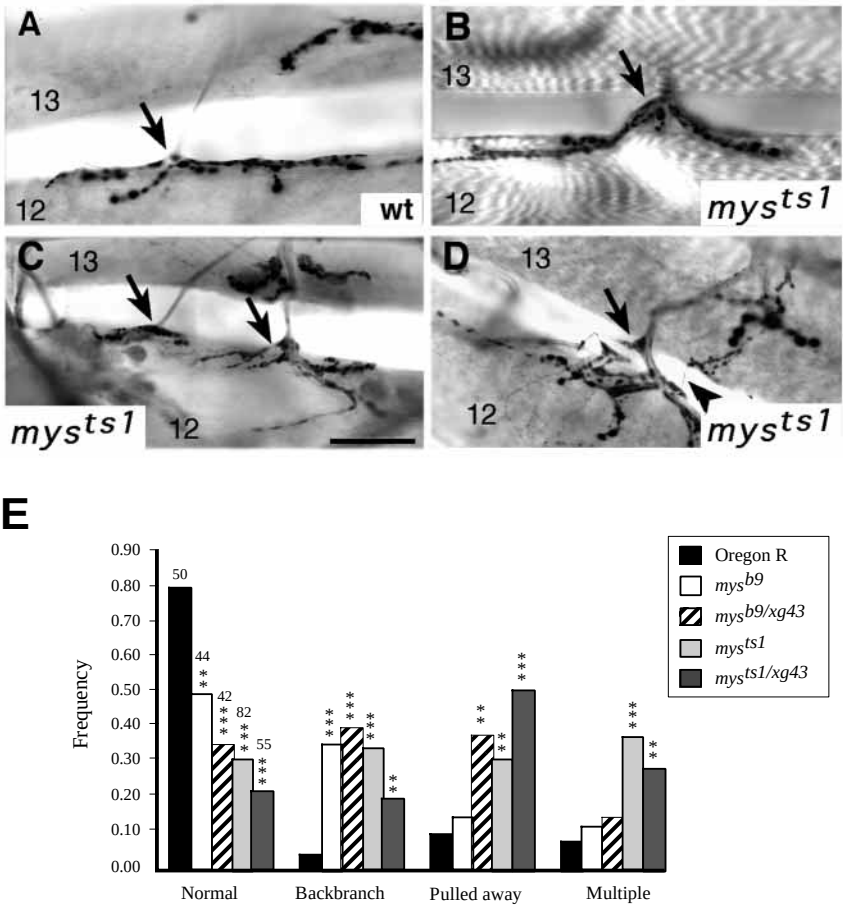

Fig. 7. Quantification of altered synapse specificity in *mys* mutant NMJs. (A) Wild-type (OR, Oregon R) muscle 12 NMJ. Arrow denotes single nerve insertion at muscle surface. (B,C) Examples of the three NMJ patterning defects quantified in *mys* mutant larvae. (B) Pulled away phenotype. Note boutons present and branching beginning above the muscle surface. (C) Multiple insertions, each denoted by an arrow. (D) Backbranching. Arrowhead indicates a branch from muscle 12 that has branched back on muscle 13. E. Quantification of each phenotype. Bars denote frequency at which a larva showed incidence of a phenotype. Numbers indicate total number of larvae of each genotype scored. Significance determined with Fishers exact test using InStat. In each genotype, animals grown at different temperatures were pooled after determining that they were not different with Fisher's Exact test (*, $P<0.05$; **, $P<0.01$; ***, $P<0.001$). Scale bar 50 μm.

Synaptic specificity is altered in βPS mutants

As errors in pathfinding have been reported in animals lacking α integrin subunits (Hoang and Chiba, 1998), 3rd instar larvae with altered integrin expression at the NMJ were examined for aberrations that might be the result of either errors in pathfinding or in synapse remodeling or maturation (Gorczyca et al., 1999). For this analysis, we chose to quantitatively assay the complex, muti-innervated muscle 12 NMJ. Three types of gross patterning abnormalities, designated as backbranched, pulled away or multiple insertions, were noted and quantified in a blind study (Fig. 7). The first of these phenotypes, backbranched, consists of at least one arboreal branch leaving muscle 12 and branching back onto muscle 13 from a site away from the point of nerve entry onto muscle 12 (Fig. 7D). This architecture was very rare in normal animals (<5%) but abnormally occurred at high levels in all *mys* mutant animals; the error is most common in mys^{b9} and mys^{b9}/mys^{XG43} (both >30%; Fig. 7E). The second phenotype, pulled away, is characterized by boutons suspended in the space between muscles 12/13, and defasciculation, or branching, beginning before the nerve has actually reached the point of insertion on the muscle (Fig. 7B). This phenotype was again rare in controls (<10%) but common in all genotypes with severely reduced βPS expression; mys^{ts1}/mys^{XG43} mutant larvae showed a 50% incidence of this defect (Fig. 7E). Finally, the third phenotype, multiple insertions, is characterized by two or more separate and distinct nerve entry points on muscle 12 (Fig. 7C). In these junctions, both nerves could frequently be traced back to a point of separation above muscle 13, though occasionally the separation would occur after the nerve had left muscle 13. The appearance of multiple nerve entry points was rare in controls (<10%) and was not significantly increased in mys^{b9} and mys^{b9}/mys^{XG43} mutants. However, multiple nerve entry points were a common consequence of severe βPS loss in both mys^{ts1} and mys^{ts1}/mys^{XG43} animals (Fig. 7E). We conclude that alterations in βPS expression also exert effects on the pattern of innervation and synaptic specificity during NMJ development.

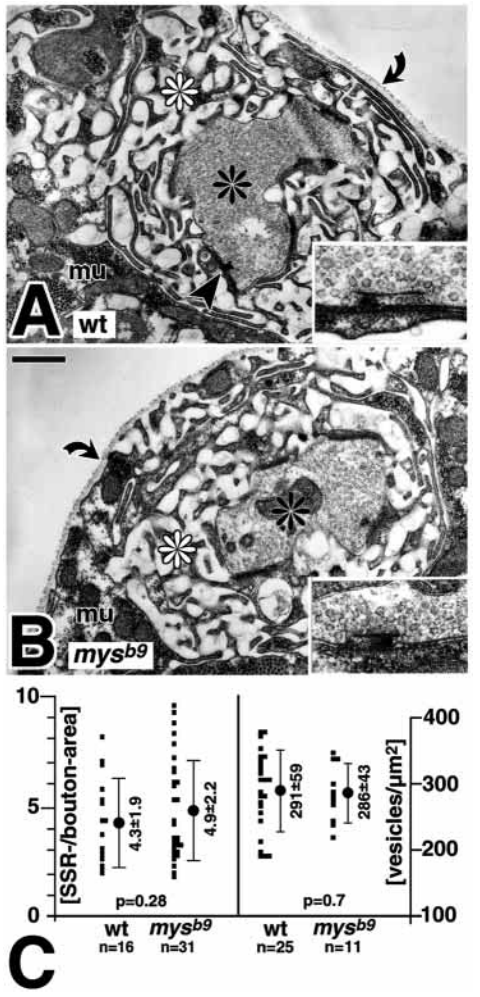

Fig. 8. Ultrastructural analyses of NMJs in wild-type and *mys* mutant larvae. Type I boutons on muscles 6/7 in wild-type (A) and mys^{b9}/mys^{XG43} mutant larvae (B) are indistinguishable with respect to presynaptic bouton size (black asterisks), vesicle density, synapse structure (close ups; with presynaptic T-bar, dashed material in the synaptic cleft and occasional omega-figures of the presynaptic membrane) and surrounding subsynaptic reticulum (SSR; white asterisks). Curved arrows point at basement membrane on the muscle (mu) surface. (C) Neither measurements of the SSR area (left; given as SSR area/bouton area) nor of vesicle density (right; given as vesicles per μm^2) of NMJs on muscles 6/7 reveal differences between wild-type and mys^{b9}/mys^{XG43}mutant larvae (mys^{b9}). Number of samples (*n*), the distribution of single measurements (black squares), mean and standard deviation (black dots with error bars and the associated numbers) and the significance (*P*) determined with a Mann-Whitney-U-test are given. Scale bar, 500 nm and 210 nm in close ups.

Synaptic ultrastructure of βPS mutants is unaffected

All three PS integrins are clearly localized to the postsynaptic SSR and their postembryonic expression correlates with the time during which SSR develops (Budnik, 1996). Therefore, we examined the ultrastructure of the larval SSR at type I NMJs in wild type and mys^{b9}/mys^{XG43}, a severe hypomorphic combination that rarely survives to adulthood (Fig. 8). Qualitatively, SSR morphology appeared unaffected (Fig. 8A,B), and quantitative measurements (see Methods) revealed no significant deviation from wild type: the SSR mean cross-section area was 5.0±3.1 μm^2 in wild-type and 4.7±2.9 μm^2 in mutant larvae (*P*=0.9; see also SSR/bouton ratio in Fig. 8C). Therefore, we conclude that SSR structural integrity is maintained despite strong reduction in βPS integrin expression.

Our immunological results suggested that βPS integrin is also present presynaptically; however, the mys^{b9}/mys^{XG43} mutant boutons appeared ultrastructurally normal (Fig. 8A,B). The *mys* synapses showed all features described for wild type (T-bars, regular material in the synaptic cleft, omega figures of the presynaptic membrane below the T-bar; see also Prokop, 1999). Likewise, the presynaptic membranes were normally attached to the postsynaptic membrane, indicating that gross membrane adhesion was unaffected. Synaptic vesicle density in *mys* mutant boutons was also indistinguishable from wild type (wild type 291±59 and mys^{b9}/mys^{XG43} mutant larvae 286±43 vesicles per μm^2; *P*=0.7; Fig. 8C). The lack of ultrastructural defects at mys^{b9}/mys^{XG43} mutant NMJs is in agreement with the lack of ultrastructural defects at synapses of *mys* null mutant embryos (Prokop et al., 1998).

Synaptic function is not strongly altered in *mys* mutant larvae

To assay whether altered mutant synaptic morphology is accompanied by altered functional synaptic transmission, we recorded nerve-evoked excitatory junctional currents (EJCs) at *mys* mutant NMJs. EJCs were recorded in physiological (1.5 mM Ca^{2+}-containing) saline in muscle 4 and muscle 6 (Fig. 9A). Visible muscle contractions were evoked in both wild-type and mutant larvae by single suprathreshold nerve stimulations (3-10 V, 0.4-0.5 mseconds). At the muscle 4 NMJ, the majority (6 of 10) of mys^{b9} larvae (reduced bouton number and branching) displayed EJC amplitudes in the normal range, while a subset (4 of 10) had unusually small EJC amplitudes (range: 96 to 111 nA; Fig. 9B) even after increasing the stimulation intensity (>20 V; not shown). Overall however, mys^{b9} mean EJC amplitude (164±57 nA, *n*=10) was only slightly reduced compared to wild type (197±42 nA; Fig. 9B). In mys^{b9}/mys^{XG43} larvae, EJC amplitudes were similarly unaffected (211±46 nA). Similarly, at the more complex muscle 6 NMJ, mys^{b9} larvae (reduced bouton number and branching) had significantly decreased EJC amplitude (182±39 nA) compared to wild type (250±35 nA, Fig. 9B), although the mys^{b9}/mys^{XG43} larvae appeared normal. By contrast, both mys^{ts1} (increased bouton number and branching) and mys^{ts1}/mys^{XG43} larvae (increased branching) had significantly larger mean EJC amplitudes at muscle 4 than wild type or mys^{b9} genotypes (Fig. 9B).

To determine whether the altered EJC amplitudes might reflect a change in quantal size, we recorded spontaneous miniature EJCs (mEJCs) in mys^{b9} and mys^{ts1} larvae (Fig. 9C). Neither mutant strain displayed altered mEJC frequency relative to wild type. Mean mEJC (quantal) amplitude was similarly unaltered in mys^{ts1} NMJs, and very slightly increased (15%; *P*<0.001) in mys^{b9}, compared to wild type. These results suggest that that alterations in MEJC frequency or amplitude cannot explain any of the changes observed in evoked neurotransmission.

In summary, the observed alterations in functional synaptic transmission in *mys* mutants are generally consistent with alterations in mutant terminal morphology. Specifically, EJC

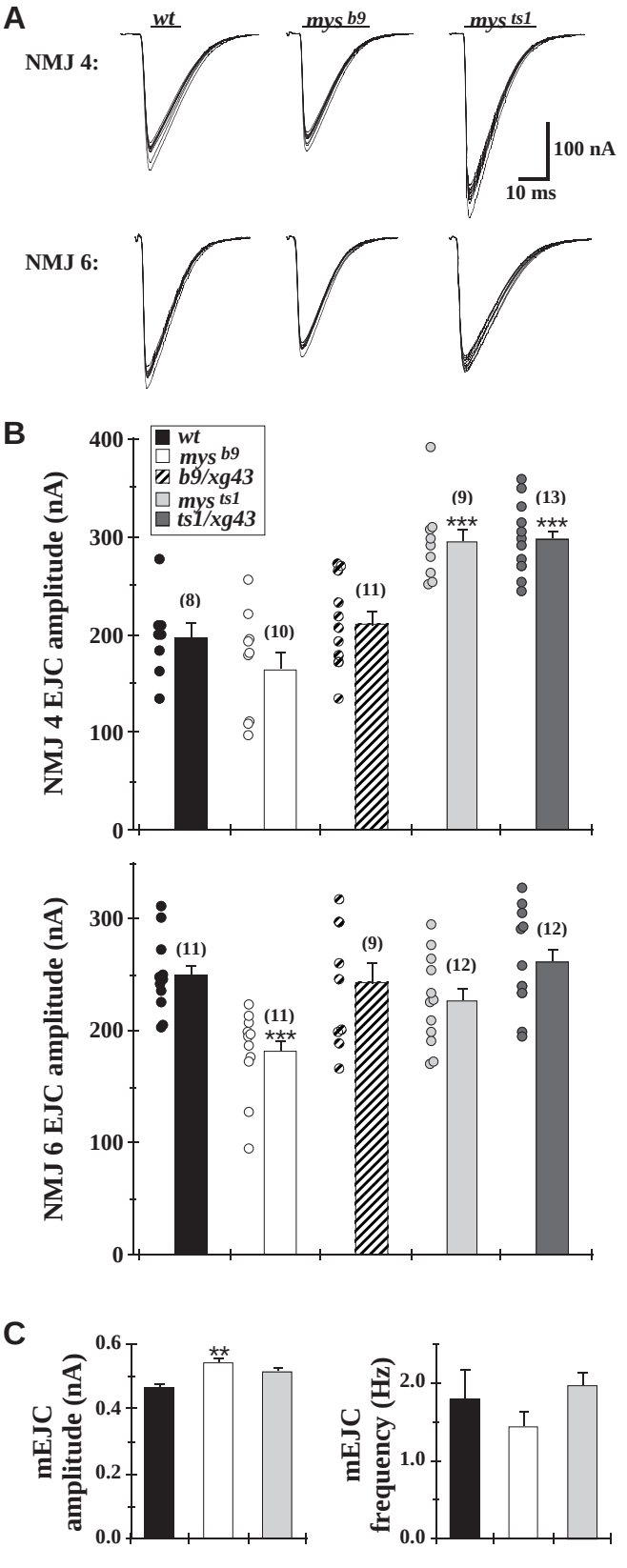

Fig. 9. Altered synaptic transmission at *mys* mutant NMJs. (A) Nerve-evoked excitatory junctional currents (EJCs; 0.2 Hz stimulation) recorded at the NMJs of muscle 6 (upper) and muscle 4 (lower) in wild-type, mys^{b9} and mys^{ts1} larvae in saline containing 1.5 mM Ca^{2+}. Each set of traces shows ten consecutive EJCs evoked at stimulus intensities that excited both low- and high-threshold motor inputs. (B) EJC peak amplitudes in muscle 4 (upper plot) and muscle 6 (lower plot) in normal and *mys* mutant larvae. Symbols indicate scatter of mean EJC amplitudes at individual NMJs; bars show overall mean EJC amplitude ± s.e.m. for each strain. Numbers of larvae analysed is indicated above bars. At muscle 4, EJC amplitudes of mys^{ts1} and mys^{ts1} /mys^{XG43} larvae are greater than those of wild-type larvae (**; $P<0.01$). At muscle 6, mys^{b9} EJC amplitude is smaller than that of both wild type (***; $P<0.001$). (C) Mean miniature EJC (mEJC) amplitude (left) and frequency (right) in muscle 4 for wild-type, mys^{b9} and mys^{ts1} larvae (1.5 mM Ca^{2+}). Mutant and wild-type terminals had comparable mEJC amplitudes (0.47±0.01 nA, wt; 0.54±0.02 nA, mys^{b9}; 0.51±0.02 nA, mys^{ts1}), though mys^{b9} amplitude is significantly greater than for wild type (**; $P<0.01$), and displayed no significant differences in mEJC frequency.

amplitudes are increased only in alleles (mys^{ts1}, mys^{ts1}/mys^{XG43}) displaying the most marked terminal overgrowth, and EJC amplitudes are decreased only in the allele (mys^{b9}) displaying the most marked terminal undergrowth. However, the functional changes recorded under these mutant conditions are relatively moderate (25-50%), and are not consistently observed at different classes of NMJs in the same mutant allele. We conclude, therefore, that integrins can modulate synaptic function in line with terminal morphology, but that this modulation is unlikely to have a profound impact on the physiology of the organism.

DISCUSSION

PS integrins are required for growth and synapse specificity at postembryonic synaptic terminals

We have shown that three integrin subunits are expressed at the *Drosophila* NMJ; two alpha subunits, αPS1 and αPS2, are expressed at least in the postsynaptic SSR membrane, and a beta subunit, βPS, is located both presynaptically and postsynaptically. Thus, at the NMJ, αPS1 and αPS2 subunits are co-localized in a single cell type, in contrast to other *Drosophila* tissues (Brown, 1993). However, the localization of multiple subunits to a single tissue is common in vertebrates (Pinkstaff et al., 1999) and has been suggested by results on PS integrin function also in *Drosophila* wing development (Brower et al., 1995). All three subunits show a specific onset of synaptic expression in postembryonic stages, and are restricted to type I boutons. Downregulation of αPS subunits in *mys* mutant alleles strongly suggests that the βPS subunit heterodimerizes with both α subunits at the NMJ. In addition to the αPS subunits, a third α integrin subunit, α-Volado, which is expressed presynaptically at the NMJ (J. R. et al., unpublished data) is a potential partner for the βPS subunit in the neuronal membrane. Thus, similar to vertebrates, *Drosophila* exhibits several integrin isoforms at the NMJ, distributed on both faces of the synaptic cleft (Martin et al., 1996).

Both *mys* mutants described here exhibit reduced βPS protein at the NMJ, frequently below detectable levels. Since both alleles have been sequenced (D. Brower, personal communication) and shown to have normal coding regions, we

suggest that this reduction is due to mutations in the complex regulatory regions of the *mys* gene. Alternatively, the defect may be in the developmental regulation of distinct splice isoforms (Zusman et al., 1993). Since α integrin subunits are reported to leave the endoplasmic reticulum only as heterodimers (Cheresh and Spiro, 1987), we were surprised to see that reduction in αPS1 and αPS2 subunit expression was less severe than the reduction of the βPS subunit. This does not seem to be due to different sensitivities of the PS antibodies since, in our hands, βPS immunological staining is more consistent and robust than any of our αPS stainings (see also Hoang and Chiba, 1998). Therefore, either αPS subunits depend only partly on heterodimerization for their synaptic localization, or there might be an as yet undiscovered β integrin subunit at the *Drosophila* NMJ. This does not seem to be the *Drosophila* β subunit βν (Yee and Hynes, 1993), since it is not detectably expressed at the NMJ.

Our observations demonstrate that the level of PS integrins at postembryonic NMJs is a critical determinant of morphological sprouting, growth and bouton differentiation. First, moderate decrease in the detection of βPS expression at the NMJ accompanied by an increase in extrasynaptic muscle expression (in mys^{b9}) results in undergrowth and compaction of the terminal, loss of boutons, a decrease in overall bouton size and the proliferation of a new class of 'mini-boutons'. Second, in contrast, severe reduction in the detection of βPS expression at the NMJ, unaccompanied by a detectable increase in extrasynaptic expression (in mys^{ts1}), results in an increase in sprouting and morphological growth to cause overgrowth and an increase in terminal complexity. Third, overexpression of βPS, generalized or nerve/muscle-specific, reduces branching complexity and bouton numbers. In agreement with the mys^{b9} observations, early βPS overexpression in the muscle also increases the frequency of mini-boutons. Thus, the subcellular distribution of βPS in both the motor neuron and its muscle partner is an important determinant of morphological development at the postembryonic NMJ.

The identity of the mini-boutons is of particular interest. Mini-boutons are found very abundantly in mys^{b9} and βPS-overexpressing terminals, but are also observed at wild-type NMJs at a low frequency (see Fig. 4A). Molecularly, these structures show the hallmarks of type I boutons but are many-fold smaller. An exciting recent study (Zito et al., 1999) using confocal imagery of live synapses has suggested that these structures may represent immature type I boutons and/or new terminal branches. Our molecular labeling defines these structures as nascent type I boutons. It appears, therefore, that decreased βPS integrin expression triggers the differentiation process for these bouton precursors, but that some subsequent condition required for maturation is not being met. Our observations suggest that proliferation of these immature type I boutons is correlated with extrasynaptic expression of βPS. Thus, we suggest that bouton formation is developmentally arrested when presented with the incorrect expression of βPS in the target membrane, leading to a failure of terminal bouton maturation.

In addition to the terminal defects, changes in βPS expression also alter distinct aspects of synapse specificity in the neuromusculature. In *mys* mutants, arboreal branches alter normal developmental paths and branch inappropriately on to non-target muscles. Moreover, the nerve often defasciculates and branching initiates from sites prior to the normal nerve entry point, and boutons differentiate in the absence of the appropriate postsynaptic target. Finally, multiple, spatially separated insertions can occur on muscles which normally have only a single, unified nerve entry point. These defects indicate that integrins may be involved in the mechanisms that identify muscle targets, and specify the particular morphology, synapse type and function of the synapse on each muscle. Recently, a potential transcription factor, *mod(mdg4)*, has been implicated in similar synaptic defects, as well as in ultrastructural defects not noted in integrin mutants (Gorczyca et al., 1999). It has been suggested that this transcription factor may regulate genes involved in the development of synapse identity. Potentially, integrins are part of the mechanisms involved in this development of identity.

The change in NMJ morphology in *mys* mutant larvae is accompanied by alterations in synaptic transmission strength. The overgrowth observed in mys^{ts1} and mys^{ts1}/mys^{XG43} mutants is accompanied by a parallel increase in transmission amplitude at some NMJs, whereas a decrease in synaptic function accompanies the undergrowth observed in mys^{b9} mutant larvae at other NMJs. This change in function is clearly in parallel to the change in NMJ morphology, but does not occur in every NMJ in every genotype. This may be consistent with βPS integrin being involved in NMJ specificity and playing different roles at different NMJs.

It is presently unclear whether the phenotypes observed in different genotypes reflects alterations in the level/distribution of βPS or interaction with other, more subtle mutations in specific genetic backgrounds. Specifically, when animals carrying either mys^{b9} or mys^{ts1} over mys^{XG43}, a null allele, were examined, we usually, but not always, observed changes in the severity of the various synaptic phenotypes. The usual case was to modify the extent of the observed phenotypes, which remained quantitatively significant although, in some cases, the phenotype disappeared entirely. There are two potential explanations for this observation. First, only a portion of the phenotype observed in the homozygous animals may be due solely to the integrin mutation, with the remainder arising from interaction with modifiers in the genetic background. Second, since both mutants are regulatory and the phenotype is most likely due not to a change in the protein but to a change in the relative distribution of the protein, making the mutant heterozygous over a protein null changes the protein distribution to a new state with novel phenotypic consequences. At this point, we are unable to distinguish between these two possibilities.

Coordinated regulation of synaptic architecture and function in *Drosophila*

In *Drosophila*, a number of mutations cause morphological changes in NMJ structural architecture. In the majority of these mutations, synaptic transmission strength is affected in parallel with NMJ size (Table 2; Budnik et al., 1996; Keshishian et al., 1996). This coupled alteration has been shown for hyperactive NMJs such as those in *Shaker ether-a-go-go* (*Sh eag*; both genes encode K^+ channel subunits) double mutants, mutants with affected second messenger pathways such as *dunce* (*dnc*, a cAMP-specific phosphodiesterase) and CaM kinase II, and

Table 2. Proteins affecting synaptic growth and expression at the *Drosophila* NMJ

Protein	Role	Expression	Growth	Function
Eag Sh	K^+ channels	mutant protein	++	++
Dunce (cAMP-phosphodiesterase)	signaling	mutant protein	++	++
CaM kinase	signaling	inhibited	++	++
Fasciclin I	adhesion	–	++	++
		++	–	–
Fasciclin II	adhesion	–	++	N/C
		–	–	N/C
βPS integrin	adhesion/ signaling	mislocalized	–	–
		reduced	++	++

In each column, + and – indicate, respectively, an increase or decrease in protein expression, growth or synaptic function. N/C, not changed.

for mutants with affected levels of the adhesion molecule Fasciclin I (Fas I). (Table 2; Zhong and Shanley, 1995; reviewed in Budnik et al., 1996; Keshishian et al., 1996). Like the above genes and regulatory components, PS integrins alter both growth and strength of transmission at the NMJs in parallel, although the degree of this coupled alteration is less striking than in these other examples.

In contrast, it has been elegantly shown that growth and synaptic strength can be genetically separated and singly regulated through independent molecular pathways (Davis et al., 1996); the adhesion molecule Fasciclin II serves as a growth regulator and the transcription factor CREB controls synaptic transmission strength. The dual activation of both pathways is required to alter NMJ structure in parallel with function (Davis et al., 1996; Table 2). A decrease in Fas II is not in itself sufficient to alter synaptic function, which requires a concurrent reduction in CREB (Davis et al., 1996). This division between growth and function is more blurred in the case of βPS mutants. On the one hand, it appears that *mys* mutations by themselves can alter function and growth in parallel. However, it is also clear that alteration in βPS expression alone is not sufficient to alter function at all junctions, and that functional phenotypes may be sensitive to genetic background. Integrins may interact with distinct sets of molecules at different junctions, affecting function in different ways.

Integrin transmembrane receptors link the extracellular matrix and the intracellular cytoskeleton, and might therefore serve either as simple adhesion molecules or as more complex signaling mediators between outer and inner cell surface (Hynes, 1992). The adhesion and signaling functions of the *Drosophila* PS integrins have been shown to be separable and to be differentially required in different tissues (Martin-Bermudo and Brown, 1999). Since the cell adhesion molecule Fas I can regulate both NMJ size and function (Zhong and Shanley, 1995), the PS integrins might similarly function as relatively simple cell adhesion molecules at the NMJ. If so, they do not appear required for maintained intercellular adhesion, since the synaptic cleft looks normal in ultrastructural analyses of *mys* mutant NMJs (Fig. 6; and Prokop et al., 1998). Integrins are more likely to modify adhesion, e.g. by interacting with other adhesion molecules, such as the fasciclins, in *cis* (Porter and Hogg, 1998). Such a modulatory role might explain both the synaptic specificity of the functional effect and the dosage dependence of PS integrins for growth control shown here, as well as the inability of the several adhesion molecules (Fas I, Fas II, integrins) found at the NMJ to compensate for one another.

Alternatively, the PS integrins could serve as transmembrane signaling molecules at the larval NMJ, independently initiating signaling pathways. One potential link of PS integrins to the regulation of NMJ growth and strength is through the CaM kinase II pathway, since reduction in CaM kinase II function results in NMJ structural defects which are strikingly similar to those documented here in *mys* mutant larvae (Table 2; Wang et al., 1994). As well, CaM kinase II is known to function in 'cross-talk', or co-regulation, between different integrin heterodimers in vertebrate macrophages (Blystone et al., 1999; Bouvard and Block, 1998). Currently, the only known targets for CaM kinase II in the terminal are Eag, a K^+ channel subunit, and Dlg, involved in localizing synaptic proteins, which may explain the alteration in transmission strength following CaM kinase II perturbation experiments (Griffith et al., 1994; Koh et al., 1999). However, potentially, CaM kinase II also targets one or more PS integrin heterodimers, activating signal cascades, mediating cross-talk, and influencing both structure and function. It seems clear that we will need to consider the integrins in light of their signal transduction features as well as their adhesion features and explore mechanisms that may link morphological and functional synapse specificity.

We thank D. Brower, N. Brown, L. Martín-Bermudo, E. Martín-Blanco, and R. Hynes for kindly providing fly stocks and antibodies. We are especially grateful to D. Brower for the unpublished *mys^{b9}* line, N. Brown for extensive assistance and insightful discussions, M. Condic for comments on this manuscript and to M. Bate in whose laboratory some of this work was initiated. We thank Keri Swearingen and Amber Bradshaw for extensive technical assistance. A.P. was funded by a Human Capital and Mobility Fellowship (European Community) and a Fellowship from the Lloyd's of London Tercentenery Foundation. K. B. and laboratory were funded by a Searle Scholarship and NSF CAREER grant.

REFERENCES

Ashburner, M. (1989). *Drosophila*. Cold Spring Harbor, NY: Cold Spring Harbor Laboratory.

Baum, P. D. and Garriga, G. (1997). Neuronal migrations and axon fasciculation are disrupted in *ina-1* integrin mutants. *Neuron* **19**, 51-62.

Bloor, J. W. and Brown, N. H. (1998). Genetic analysis of the *Drosophila* αPS2-integrin subunit reveals discrete adhesive, morphogenetic and sarcomeric functions. *Genetics* **148**, 1127-1142.

Blystone, S. D., Slater, S. E., Williams, M. P., Crow, M. T. and Brown, E. J. (1999). A molecular mechanism of integrin crosstalk: alphavbeta3 suppression of calcium/calmodulin-dependent protein kinase II regulates alpha5beta1 function. *J. Cell Biol.* **145**, 889-897.

Bogaert, T., Brown, N. and Wilcox, M. (1987). The *Drosophila* PS2 antigen is an invertebrate integrin that, like the fibronectin receptor, becomes localized to muscle attachments. *Cell* **51**, 929-940.

Bouvard, D. and Block, M. R. (1998). Calcium/calmodulin-dependent protein kinase II controls integrin alpha5beta1-mediated cell adhesion through the integrin cytoplasmic domain associated protein-1alpha. *Biochem. Biophys. Res. Commun.* **252**, 46-50.

Brabant, M. C. and Brower, D. L. (1993). PS2 integrin requirements in *Drosophila* embryo and wing morphogenesis. *Dev. Biol.* **157**, 49-59.

Broadie, K. S. and Bate, M. (1993). Development of the embryonic neuromuscular synapse of *Drosophila melanogaster*. *J. Neurosci.* **13**, 144-166.

Brower, D. L., Bunch, T. A., Mukai, L., Adamson, T. E., Wehrli, M., Lam, S., Friedlander, E., Roote, C. E. and Zusman, S. (1995). Nonequivalent

requirements for PS1 and PS2 integrin at cell attachments in *Drosophila*: genetic analysis of the alpha PS1 integrin subunit. *Development* **121**, 1311-1320.

Brower, D. L., Wilcox, M., Piovant, M., Smith, R. J. and Reger, L. A. (1984). Related cell-surface antigens expressed with positional specificity in *Drosophila* imaginal discs. *Proc. Natl Acad. Sci. USA* **81**, 7485-7489.

Brown, N. H. (1993). Integrins hold *Drosophila* together. *BioEssays* **15**, 383-389.

Budnik, V. (1996). Synapse maturation and structural plasticity at *Drosophila* neuromuscular junctions. *Curr. Opin. Neurobiol.* **6**, 858-867.

Budnik, V., Koh, Y. H., Guan, B., Hartmann, B., Hough, C., Woods, D. and Gorczyca, M. (1996). Regulation of synapse structure and function by the *Drosophila* tumor suppressor gene *dlg*. *Neuron* **17**, 627-640.

Budnik, V., Zhong, Y. and Wu, C. F. (1990). Morphological plasticity of motor axons in *Drosophila* mutants with altered excitability. *J. Neurosci.* **10**, 3754-3768.

Bunch, T. A., Salatino, R., EngelgjesdM. C., Mukai, L., West, R. F. and Brower, D. L. (1992). Characterization of mutant alleles of *myospheroid*, the gene encoding the β-subunit of the *Drosophila* PS integrins. *Genetics* **132**, 519-528.

Burkin, D. J., Gu, M., Hodges, B. L., Campanelli, J. T. and Kaufman, S. J. (1998). A functional role for specific spliced variants of the alpha7beta1 integrin in acetylcholine receptor clustering. *J. Cell Biol.* **143**, 1067-1075.

Chen, B. M. and Grinnell, A. D. (1995). Integrins and modulation of transmitter release from motor nerve terminals by stretch. *Science* **269**, 1578-1580.

Cheresh, D. A. and Spiro, R. C. (1987). Biosynthetic and functional properties of an Arg-Gly-Asp-directed receptor involved in human melanoma cell attachment to vitronectin, fibrinogen, and von Willebrand factor. *J. Biol. Chem.* **262**, 17703-17711.

Chiba, A. and Keshishian, H. (1996). Neuronal pathfinding and recognition: roles of cell adhesion molecules. *Dev. Biol.* **180**, 424-432.

Davis, G. W., Schuster, C. M. and Goodman, C. S. (1996). Genetic dissection of structural and functional components of synaptic plasticity. III. CREB is necessary for presynaptic functional plasticity. *Neuron* **17**, 669-679.

Fassler, R., Georges-Labouesse, E. and Hirsch, E. (1996). Genetic analyses of integrin function in mice. *Curr. Opin. Cell Biol.* **8**, 641-646.

Fernandes, J. J., Celniker, S. E. and VijayRaghavan, K. (1996). Development of the indirect flight muscle attachment sites in *Drosophila*: Role of the PS-integrins and the *stripe* gene. *Dev. Biol.* **176**, 166-184.

Flybase. (1998). Flybase: A *Drosophila* database. *Nucleic Acids Res.* **26**, 85-88.

Gorczyca, M., Popova, E., Jia, X. X. and Budnik, V. (1999). The gene mod(mdg4) affects synapse specificity and structure in Drosophila. *J. Neurobiol.* **39**, 447-460.

Griffith, L. C., Wang, J., Zhong, Y., Wu, C. F. and Greenspan, R. J. (1994). Calcium/calmodulin-dependent protein kinase II and potassium channel subunit Eag similarly affect plasticity in *Drosophila*. *Proc. Natl Acad Sci. USA* **91**, 10044-10048.

Grotewiel, M. S., Beck, C. D., Wu, K. H., Zhu, X. R. and Davis, R. L. (1998). Integrin-mediated short-term memory in *Drosophila*. *Nature* **391**, 455-460.

Hoang, B. and Chiba, A. (1998). Genetic analysis of the role of integrin during axon guidance in *Drosophila*. *J. Neurosci.* **18**, 7847-7855.

Huang, A. M., Wang, H. L., Tang, Y. P. and Lee, E. H. (1998). Expression of integrin-associated protein gene associated with memory formation in rats. *J. Neurosci.* **18**, 4305-4313.

Hynes, R. O. (1992). Integrins: versatility, modulation, and signaling in cell adhesion. *Cell* **69**, 11-25.

Hynes, R. O. (1996). Targeted mutations in cell adhesion genes: what have we learned from them? *Dev. Biol.* **180**, 402-412.

Jan, L. Y. and Jan, Y. N. (1976). Properties of the larval neuromuscular junction in *Drosophila melanogaster*. *J. Physiol.* **262**, 189-214.

Johansen, J., Halpern, M. E., Johansen, K. M. and Keshishian, H. (1989). Stereotypic morphology of glutamatergic synapses on identified muscle cells of *Drosophila* larvae. *J. Neurosci.* **9**, 710-725.

Keshishian, H., Broadie, K., Chiba, A. and Bate, M. (1996). The *Drosophila* neuromuscular junction: a model system for studying synaptic development and function. *Annu. Rev. Neurosci.* **19**, 545-575.

Koh, Y. H., Popova, E., Thomas, U., Griffith, L. C. and Budnik, V. (1999). Regulation of DLG localization at synapses by CaMKII-dependent phosphorylation. *Cell* **98**, 353-363.

Leptin, M., Bogaert, T., Lehmann, R. and Wilcox, M. (1989). The function of PS-integrins during *Drosophila* embryogenesis. *Cell* **56**, 401-408.

Lindsley, D. L. and Zimm, G. (1992). *The Genome of Drosophila melanogaster.* San Diego: Academic Press.

Martin, P. T., Kaufman, S. J., Kramer, R. H. and Sanes, J. R. (1996). Synaptic integrins in developing, adult, and mutant muscle: selective association of alpha1, alpha7A, and alpha7B integrins with the neuromuscular junction. *Dev. Biol.* **174**, 125-139.

Martin-Bermudo, M. D. and Brown, N. H. (1999). Uncoupling integrin adhesion and signaling: the βPS cytoplasmic domain is sufficient to regulate gene expression in the *Drosophila* embryo. *Genes Dev.* **13**, 729-739.

Pinkstaff, J. K., Detterich, J., Lynch, G. and Gall, C. (1999). Integrin-subunit gene expression is regionally differentiated in adult brain. *J. Neurosci.* **19**, 1541-1556.

Porter, J. C. and Hogg, N. (1998). Integrins take partners: cross-talk between integrins and other membrane receptors. *Trends Cell Biol.* **8**, 390-396.

Prokop, A. (1999). Integrating bits and pieces – synapse formation in *Drosophila* embryos. *Cell Tissue Res.* **297**,169-186.

Prokop, A., Martin-Bermudo, M. D., Bate, M. and Brown, N. H. (1998). Absence of PS-integrins or laminin A affects extracellular adhesion, but not intracellular assembly, of hemiadherens and neuromuscular junctions in *Drosophila* embryos. *Dev. Biol.* **196**, 58-76.

Rohrbough, J., Pinto, S., Mihalek, R., Tully, T. and Broadie, K. (1999). *Latheo*, a *Drosophila* gene involved in learning, regulates functional synaptic plasticity. *Neuron* **23,** 55-70

Schmidt, C. E., Dai, J., Lauffenburger, D. A., Sheetz, M. P. and Horwitz, A. F. (1995). Integrin-cytoskeletal interactions in neuronal growth cones. *J. Neurosci.* **15**, 3400-3407.

Staubli, U., Vanderklish, P. and Lynch, G. (1990). An inhibitor of integrin receptors blocks long-term potentiation. *Behav. Neural Biol.* **53**, 1-5.

Volk, T., Fessler, L. I. and Fessler, J. H. (1990). A role for integrin in the formation of sarcomeric cytoarchitecture. *Cell* **63**, 525-536.

Wang, J., Renger, J. J., Griffith, L. C., Greenspan, R. J. and Wu, C. F. (1994). Concomitant alterations of physiological and developmental plasticity in *Drosophila* CaM kinase II-inhibited synapses. *Neuron* **13**, 1373-1384.

Woods, D. F. and Bryant, P. J. (1991). The *discs-large* tumor suppressor gene of *Drosophila* encodes a guanylate kinase homolog localized at septate junctions. *Cell* **66**, 451-464.

Yee, G. H. and Hynes, R. O. (1993). A novel, tissue-specific integrin subunit, beta nu, expressed in the midgut of *Drosophila melanogaster*. *Development* **118**, 845-858.

Zhong, Y. and Shanley, J. (1995). Altered nerve terminal arborization and synaptic transmission in *Drosophila* mutants of the cell adhesion molecule fasciclin I. *J. Neurosci.* **15**, 6679-6687.

Zinsmaier, K. E., Hofbauer, A., Heimbeck, G., Pflugfelder, G. O., Buchner, S. and Buchner, E. (1990). A cysteine-string protein is expressed in retina and brain of *Drosophila*. *J. Neurogenet.* **7**, 15-29.

Zito, K., Parnas, D., Fetter, R. D., Isacoff, E. Y. and Goodman, C. S. (1999). Watching a synapse grow: noninvasive confocal imaging of synaptic growth in Drosophila. *Neuron* **22**, 719-729.

Zusman, S., Grinblat, Y., Yee, G., Kafatos, F. C. and Hynes, R. O. (1993). Analyses of PS-integrin functions during *Drosophila* development. *Development* **118**, 737-750.